# SEASONAL PERFORMANCE SIMULATION OF A GAS-FIRED CHEMISORPTION HEAT PUMP FOR RESIDENTIAL HEA TING IN COLD CLIMATE

Zhiyao Yang[1,2], Ming Qu[1], Kyle R. Gluesenkamp[2]
[1] Purdue University, West Lafayette, IN
[2]Oak Ridge National Laboratory, Oak Ridge, TN

## ABSTRACT

Gas-fired chemisorption heat pump (CSHP) is a promising technology for high-efficiency cold-climate residential heating. The CSHP utilize the heat of reversible chemical reactions between sorbent and refrigerant to extract heat from cold ambient and supply high-temperature heat to the indoors. The energy efficiency and heating capacity of CSHP depends on the ambient temperatures and operating controls. This study evaluates the seasonal performance of a CSHP by first developing a dynamic system model and generating a performance map for various ambient and heat-supply temperatures; then the bin method is used to evaluate the CSHP seasonal peformance in two cold-climate locations for space and water heating.

## INTRODUCTION

Residential buildings accounted for 21.8% of total energy consumption in the United States in 2014 (DOE 2014). Among all end-uses in residential buildings, space and water heating are the major energy consumers, especially in cold climates where heating is in high demand. According to the Residential Energy Consumption Survey (RECS) conducted by the Energy Information Agency (EIA) in 2015, space and water heating consumed over 60% of site energy nationwide.

Figure 1 shows the main heating equipment and energy source by climate region from the same EIA report. Over 80% of the 42 million households in cold and very cold climates in the country acquire heating by combustion of natural gas and other fuels, leaving less than 20% of them relying on electric-resistance or electric-driven heat pumps for heating purposes. Therefore, developing highly efficient heating equipment especially for cold climates has significant energy saving potential. However, existing heating systems that are used in low-ambient conditions have seen major obstacles in improving their energy efficiency.

Thermally-driven ammonia-based chemisorption heat pumps (CSHP) have the potential to provide space heating with high energy efficiency in cold climates. In a CSHP, ammonia vapor is adsorbed or desorbed on the solid sorbent surface through reversible chemical reactions, and the associated reaction heat is used for heat extraction from the ambient or heat supply to the buildings. Therefore, CSHP is able to produce heating with thermal efficiency surpassing the theoretical limit of gas-fired furances and boilers

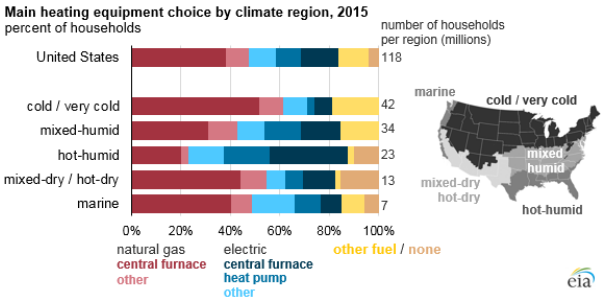


*Figure 1 Heating equipment choice by climate region (EIA 2015)*

The configuration and operation of a typical single-effect CSHP cycle with combined condenser-evaporator (CCE) similar to the one in this study is shown in Figure 2. During desorption mode, the salt in the adsorber is heated by a natural gas burner via water heat pipe. The ammonia vapor released from the salt condensates in the condenser, supplying heat to the indoor. In the adsorption mode, sensible heat of the hot adsorber and the heat from absorption reaction of the sorbent salt is extracted by circulating liquid water through the heat pipe heat exchanger, and the heat is further transferred

*This manuscript has been authored in part by UT-Battelle, LLC, under contract DE-AC05-00OR22725 with the US Department of Energy (DOE). The US government retains and the publisher, by accepting the article for publication, acknowledges that the US government retains a nonexclusive, paid-up, irrevocable, worldwide license to publish or reproduce the published form of this manuscript, or allow others to do so, for US government purposes. DOE will provide public access to these results of federally sponsored research in accordance with the DOE Public Access Plan (http://energy.gov/downloads/doe-public-access-plan).*

through a secondary loop from the heat pipe to the building. Once cooled, the dry salt in the adsorber starts to absorb ammonia vapor, resulting in continuous evaporation of liquid ammonia in the evaporator which cools the HTF in the evaporator coil. The cooled HTF in turn transfers heat from the cold ambient to the evaporator. The CSHP system continuously supplies heat to the indoor by repeating the desorption-adsorption mode.

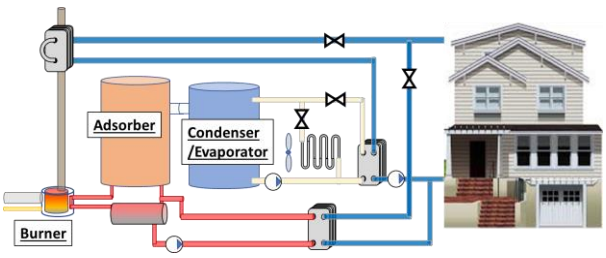


*Figure 2 configuration of a CSHP system*

Since the CSHP extracts heat from the ambient via the heat pumping effect, its performance is affected by the ambient temperature. On the other hand, the building heating load also varies with the ambient temperature. Therefore, when providing heating to a residential building, the heating capacity of a CSHP is likely to diviate from the building heating load under different ambient conditions as shown in Figure 3.

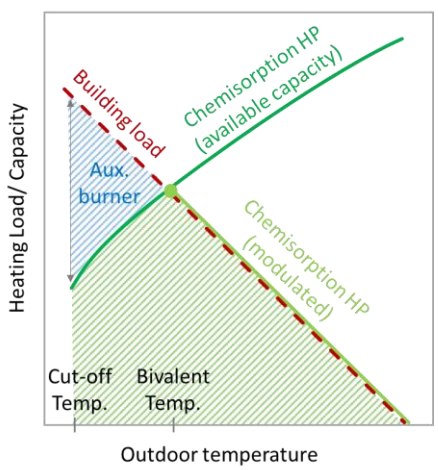


*Figure 3 Heating load and CSHP capacity under various ambient temperatures*

With the ambient temperature decreasing, the heating load of the building increasses; meanwhile, ammonia in the evaporator of the CSHP needs to evaporate at a lower pressure and temperature to extract heat from the cold ambient, reducing the heating capacity of the CSHP. The bivalent temperature is defined as the ambient temperature at which the CSHP heating capacity equals to the building heating load. At above the bivalent temperature, the heating output of the CSHP can be modulated down to satisfy the building load. Once the CSHP heating capacity becomes lower than the building load, auxiliary heating is necessary to fill the gap.

Therefore, in order to evaluate the seasonal performance of the CSHP system for residential buildings in the cold climate, the heating capacity and energy efficiency of the CSHP under various ambient temperatures need to be evaluated and combined with the building heating load to determine the annual system heating performance.

In this study, a dynamic system model is first develoepd to evaluate the system heating capacity and COP under different ambient temperatures and operating controls to generate the performance map. Then the performance map is combined with the building heating loads in cold climates to evaluate the system's seasonal performance.

## DYNAMIC CSHP SIMULATION

A dynamic model for the CSHP system is developed to evaluate the system performance under different operating conditions. The core of the gas-fired CSHP system shown in Figure 2 is the adsorber-condenser/evaporator module (sorption module), and their transient behaviors are simulated by a system of time-dependent differential equations described below. For the natural gas burner, flue gas heat exchanger, and peripheral heat exchangers, simplified steady-state performance is assumed as described with the boundary conditions.

To simplify the simulation of the sorption module, following assumptions are made:

- Uniform temperature in the adsorber.
- Unlimited mass transfer in the sorption module, therefore all sorbent is under uniform vapor pressure.
- the vapor pressure in the sorption module is determined by the saturation pressure of the condenser/evaporator.
- The heat capacities of all materials are constant regardless of the temperature.
- The amount of ammonia evaporation and condensation in the condenser/evaporator corresponds to the absorption and desorption in the adsorber, i.e. neglect the vapor ammonia accumulation in the sorption module.

The governing equations for the adsorber include chemical equilibrium, chemical kinetics, and energy balance. The equilibrium of the chemisorption reaction

can be described using the van't Hoff equation as in Eqn. (1):

$$\ln(P_{eq}) = -\frac{\Delta H_r}{RT_{salt}} + \frac{\Delta S_r}{R} \quad (1)$$

In the equations, $R$ is the gas constant, and $\Delta H_r$ and $\Delta S_r$ are the enthalpy and entropy associated with the reaction. For the particular reactions of interest:

$$LiCl \cdot 3NH_3(s) \rightarrow LiCl \cdot 2NH_3(s) + NH_3(g)$$

$$LiCl \cdot 2NH_3(s) \rightarrow LiCl \cdot 1NH_3(s) + NH_3(g)$$

$$LiCl \cdot 1NH_3(s) \rightarrow LiCl(s) + NH_3(g)$$

The $\Delta H_r$ and $\Delta S_r$ are reported in literature (Neveu et al. 1993, Li et al 2014) as listed in Table 1:

*Table 1 Properties of the ammoniate LiCl Sorbent*

| REACTION | $\Delta H_r$ [KJ/MOL] | $\Delta S_r$ [KJ/MOL-K] |
|---|---|---|
| LiCl-3/2NH3 | 44780 | 229.8 |
| LiCl-2/1NH3 | 48128 | 230.6 |
| LiCl-1/0NH3 | 51894 | 234.4 |

Based on the equilibrium equation and coefficients, the reaction equilibrium can be illustrated on Clapeyron chart in Figure 4 with the sorbent temperature as the x-axis and the equilibrium vapor pressure as the y-axis.

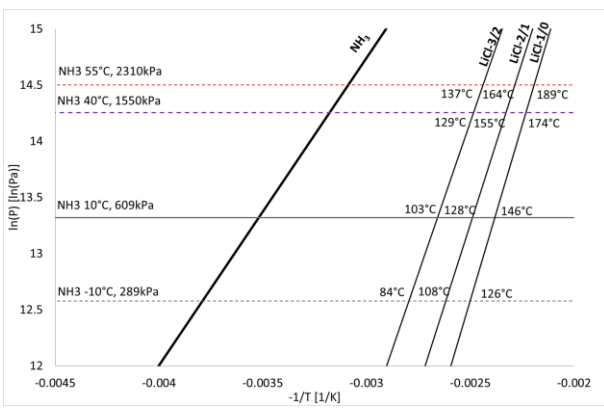


*Figure 4 Ammonia-LiCl reaction equilibrium*

To describe the chemisorption reaction kinetics, the semi-empirical reaction kinetic equation first developed by Tykodi et al. 1979 based on the classic chemical reaction kinetic equation for homogeneous reactants is used in this study. The kinetic equation is often expressed as Eqn. (2):

$$\frac{dX}{dt} = (1-X)^n \cdot Ar \cdot \ln\left(\frac{P_{eq}(T_{salt})}{P_{ads}}\right) \quad (2)$$

With the empirically identified reaction order $n$ and the Arrhenius term $Ar$, and based on the current reaction progression $X$ and the difference between the local pressure $P_{local}$ and equilibrium pressure corresponding to the salt temperature, the reaction rate can be calculated using the kinetic equation.

The change reaction progression $X$ is determined by the amount of available reactant as expressed in Eqn. () and is in turn associated with the amount of ammonia getting released or absorbed. $i$ and $j$ in Eqn. (3) represent the state of ammoniation, i.e. the amount of ammonia absorbed by the salt.

$$X_{i\rightarrow j} = \frac{N_j}{N_i + N_j} \quad (3)$$

With the chemical reaction calculated, the energy balance in the sorbent can be expressed below as Eqn. (4):

$$\frac{dT_{salt}}{dt} \cdot (Cp_{salt} \cdot m_{salt} + Cp_{HX,ads} \cdot m_{HX,ads}) = \dot{Q}_{HX,ads} - \sum \frac{dN_{i\rightarrow j}}{dt} \cdot \Delta H_{r,i\rightarrow j} \quad (4)$$

For the integrated condenser/evaporator, the mass balance of the liquid ammonia is associated with the ammonia is calculated in Eqn. (5):

$$\frac{dm_{liq}}{dt} = \sum \frac{dN_{i\rightarrow j}}{dt} \cdot M_{NH3} \quad (5)$$

The energy balance between the liquid ammonia, the condenser/evaporator heat exchanger metal, and the external heat transfer fluid is expressed in Eqn. (6):

$$\frac{dT_{liq}}{dt} \cdot (Cp_{liq} \cdot m_{liq} + Cp_{HX,CE} \cdot m_{HX,CE}) = \dot{Q}_{HX,CE} - \sum \frac{dN_{i\rightarrow j}}{dt} \cdot M_{NH3} \cdot T_{salt} \cdot Cp_{vap} \quad (6)$$

$\dot{Q}_{HX,CE}$ is calculated based on the lquid ammonia temperature and the heat transfer fluid temperature uder a constant UA and flow rate.

The boundary conditions for the CSHP system simulation are:

- The combustion efficiency of the burner is 98%, with 70% of combustion heat supplied to the adsorber, and 75% of the rest in the flue gas is recovered.
- The maximum natural gas input power is 15kW, which is modulated down when the salt temperature approaches the limit of 210°C/410°F;
- The hot water returing to the system is kept constant at 55°C/131°F.

- The desorption process is terminated and the system swithes to adsorption mode once the heating power of the condenser and the flue gas recovery combined is lower than the controlled minimum heating capacity;
- The adsorption process is terminated once the heating power of the adsorber is lower than the controlled minimum heating capacity;
- The temperature of the HTF entering the evaporator during the adsorption mode is 10°C/18°F lower than the ambient air temperature.

The initial temperatures of materials in the adsorber are all at the hot water return temperature, and those in the condenser-evaporator are at the ambient temperature to reflect the end state of a complete cycle. The initial sorbent is all LiCl-3$NH_3$, and no liquid ammonia is in the condenser-evaporator.

## CYCLE SIMULATION AND SYSTEM PERFORMANCE MAP

Cycle simulations are carried out using the dynamic system model described above on a CSHP system. The dimensions of the simulated system are listed in Table 2.

*Table 2 Dimensions of the simulated CSHP*

| ITEM | VALUE | UNIT |
|---|---|---|
| Adsorber salt mass | 2.2 | kg |
| Adsorber metal mass | 24 | kg |
| Condenser-evaporator metal mass | 24 | kg |
| Condenser-evaporator UA value | 800 | W/K |
| Maximum natural gas input | 15 | kW |
| Burner combustion efficiency | 98 | % |
| Burner-CSHP heat efficiency | 70 | % |
| Flue gas heat recovery efficiency | 75 | % |

The system dynamic simulated under the rating condition of -10°C is shown in Figure 5. With the minimum heating rate set at 2.5 kW, the desorption mode lasted for 2543s, and the sorption mode lasted for 2391s. Most of the heating output during the desorption mode is from the flue gas, with some condensation heat from the CSHP. The sorption mode sees higher dynamic with significant heating output at the start which quickly decreases later in the mode. The total gas heat input to the system is 22780 kJ, and the total heating output is 26881 kJ. The gas COP is 1.18, and the average heating capacity over the entire desorption-sorption cycle is 5.6 kW.

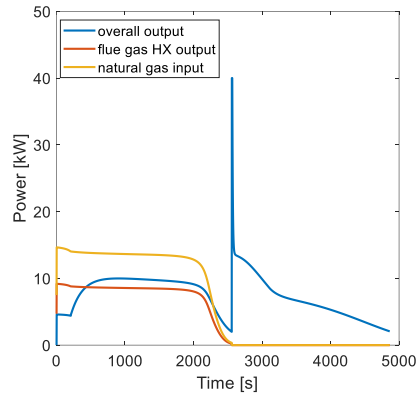


*Figure 5 dynamic gas input and heating output of the CSHP system*

Figure 6 illustrates the dynamic heating output when the heating output is controlled to be above 1-4 kW. A higher minimum limit of heating output makes the cycle shorter, with earlier switching from desorption to sorption and earlier termination of the sorption mode. Switching the mode at a higher heating output increases the system average heating capacity while on the other hand reduces the system COP, as the desorption and sorption processes are not complete when the reaction rates are still high.

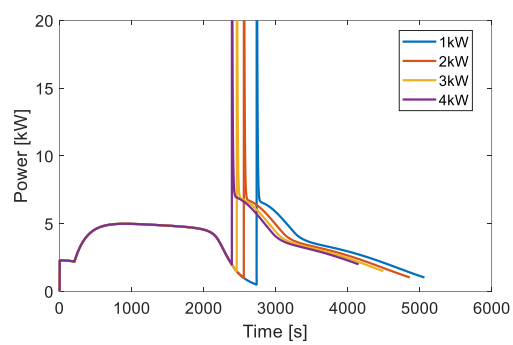


*Figure 6 dynamic heating output with controlled minimal heating rate of 1-4 kW*

The trade-off between the system heating capacity and the system heating COP under different controlled minimal heating rates is illustrated in Figure 7. As the result, when the CSHP heating capacity is modulated to match a lower building load, it benefits from the reduced demand with a higher COP.

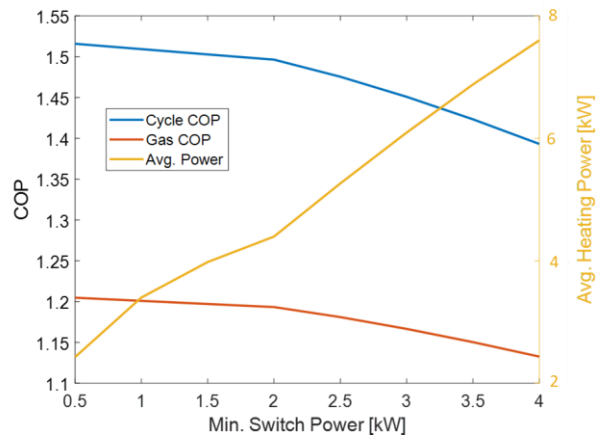


*Figure 7 Cycle and gas COP and average heating capacity under different minimal heating rate*

In order to quickly calculate the system COP for seasonal performance evaluation, a series of simulations were carried out using the dynamic model to generate a performance map for the CSHP system under different ambient temperatures and heating capacities as shown in Figure 8. Each curve Figure 8 is plotted by running the simulation under the same ambient temperature and varying the heating output. Generally the system COP benefits from lower heating capacities, which allow longer cycle time and subquently more complete chemisorption reactions and fully utilization of the heat input. On the other hand, more frequent switching between desorption and adsorption modes is required to sacrifice complete reaction for the higher heating output at the start of each mode. Such tradeoff is particularly menifested by the quick drop of COP at heating capacity above the rating capacity of 6 kW.

As shown in Figure 8, the system efficiency is consistently high at around 1.3 under heating output below 6 kW. On the other hand, with low ambient temperatures down to -25°C, the system efficiency suffers from increasing difficulty to extract heat from the colder outdoor.

Since the system thermal efficiency drops below 1.0 under sub-freezing temperatures with above 6kW heating capacity, which is not competetive compared with condensing boilers, the CSHP heating output is limited to below 6 kW.

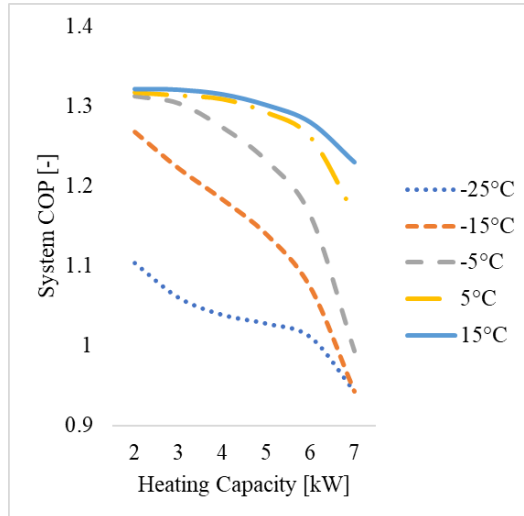


*Figure 8 CSHP cycle COP under various ambient temperatures and heating capacities*

As shown in Figure 8, the CSHP system is able to provide efficient heating under the rating capacity and moderately low ambient temperature. Although its performance decreases under large capacity and extremely cold temperatures of -25°C, it remains more efficient than conventional technologies.

## SEASONAL CSHP PERFORMANCE

With the system COP map under different ambient conditions and heating outputs, the seasonal system performance can be evaluated using the bin method along with climate data and building load simulation.

The energy used to drive the CSHP is calculated from the heating output of the CSHP and its COP as in Eqn. (7):

$$Q_{CSHP} = \sum \frac{\dot{q}_{CSHP}}{COP_{CSHP}} \tag{7}$$

If the CSHP output is not enough to cover the entire heating load (e.g. for NYC the heating output is limited within 6kW to maintain high efficiency), an auxilary condensing boiler with gas COP of 95% is used to fill the gap, and its gas consumption is calculated in Eqn. (8):

$$Q_{aux} = \sum \frac{\dot{q}_{tot} - \dot{q}_{CSHP}}{COP_{aux}} \tag{8}$$

Thus The seasonal heating COP is calculated as in Eqn (9):

$$SCOP = \frac{\sum \dot{q}_{tot}}{Q_{CSHP} + Q_{aux}} \quad (9)$$

Two typical locations in the cold climate in the U.S. investigated in Blackman et al. 2019 are selected in this study for the seasonal performance evaluation:

- New York City, NY, representative of mixed-humid climate with HDD<3000;
- Minneapolis, MN, representative of a cold-humid climate with 4000<HDD<5000.

The outdoor air temperature and bin hours for both locations are shown in Figure 9.

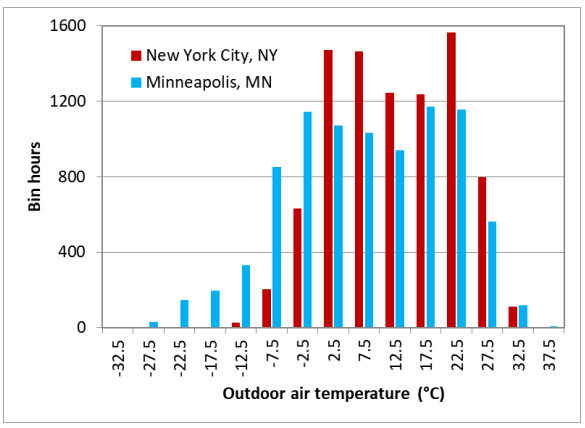


*Figure 9 Ambient temperature bins for New York City, NY and Minneapolis, MN*

Blackman et al. simulated the heating load of typical residential buildings using the 2006 IECC prototype building models (IECC, 28). The simulated building is a two-story, 223 m2(2400 ft2) single-family house with a vented attic. The simulated peak space heating load and annual space heating load is 13.4kW, 20898kWh for New York City, and 10.3kW and 16435kWh for Minneapolis. The simulated space heating loads for the two locations corresponding to different outdoor temperatures are illustrated in Figure 10. Based on the conclusion of Blackman et al., the economically optimal size of the CSHP is about 42% and 41% of the peak heating load in New York City and Minneapolis, respectively. Therefore, the rated capacity of the CSHP to supply heating to the simulated building is 5.6kW and 4.2 kW. The performance map developed in the previous section can thus be directly used for New York City case, and a CSHP with reduced capacity but similar energy efficiency profile is used for the Minneapolis case.

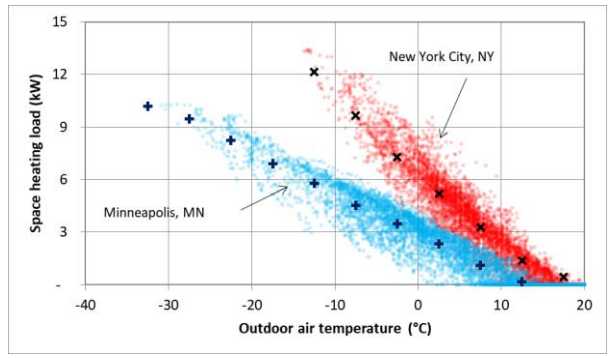


*Figure 10 Simulated space heating load under different outdoor temperatures*

Applying the performance map to the hourly temperature and heating load of New York City and Minneapolis yields the system COP over an entire year as shown in Figure 11 and Figure 12, respectively.

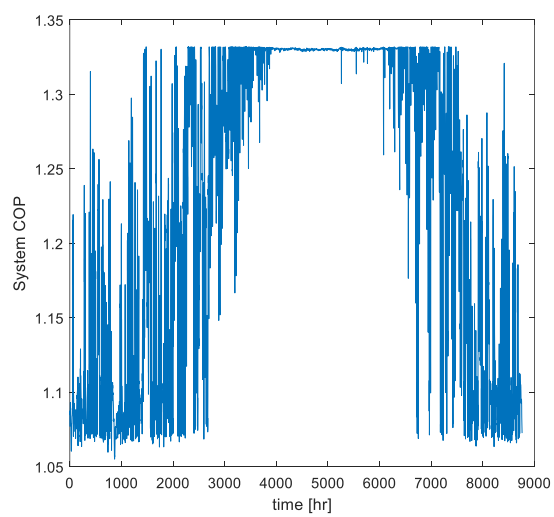


*Figure 11 Annual hourly CSHP system COP for NYC*

Using Eqn. (9) the seasonal heating COP for New York City and Minneapolis are 1.1015 and 1.0781, respectively. The fraction of auxillary heating are 11% and 5% in the total heating capacity for the two locations. The proportion of auxillary heating in Minneapolis is lower than in New York City due to the less flucturation of heaing load throughout the heating seasons, thus the heat pump capacity matches better with the load and less auxillary is required. The seasonal heating COP are 16% and 13% higher than conventional condensing boiler's 95% fuel efficiency.

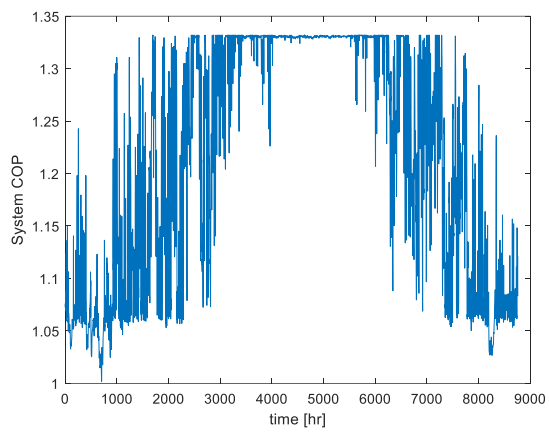


*Figure 12 Annual hourly CSHP system COP for MN*

## CONCLUSION

This study investigated the seasonal performance of chemisorption heat pump (CSHP) system for residential space heating in cold climate. First a dynamic system model for the CSHP was developed to describe the transient response of the adsorber-condenser/evaporator sorption module. Then the dynamic system model is used to generate performance map under various ambient temperatures and heating power outputs. The performance map was later used to determine the heating energy efficiency of the system for two simulated residential buildings in two typical cold-climate cities in the U.S. The CSHP demonstrated high efficiency over the entire year and achieved 16% and 13% COP improvement compared with the conventional condensing boiler.

## ACKNOWLEDGMENT

This work was sponsored by the U.S. Department of Energy's Building Technologies Office (BTO) under Contract No. DE-AC05-00OR22725 with UT-Battelle, LLC. The author also acknowledge Mr. Antonio Bouza, Technology Manager for HVAC&R, Water Heating, and Appliance, U.S. Department of Energy BTO.

## NOMENCLATURE

| | |
|---|---|
| $Ar$ | Arrhenius term for chemical reaction [-] |
| $COP$ | coefficient of performance |
| $Cp$ | specific heat [kJ/kg-K] |
| $\Delta H_r$ | reaction enthalpy [kJ/mol] |
| $\Delta S_r$ | reaction entropy [kJ/mol-K] |
| $m$ | mass [kg] |
| $M$ | molar mass [g/mol] |
| $n$ | pseudo-order of the chemical reaction [-] |
| $N$ | number of moles [mol] |
| $P$ | pressure |
| $\dot{Q}$ | heat transfer rate [kW] |
| $\dot{q}$ | hourly heat load [kJ] |
| $Q$ | total heat transfer [kJ] |
| $R$ | gas constant [kJ/kmol-K] |
| $SCOP$ | seasonal coefficient of performance |
| $T$ | temperature [K] |
| $X$ | reaction progression [-] |

**Subscripts**

| | |
|---|---|
| $ads$ | adsorber |
| $aux$ | auxiliary boiler |
| $CE$ | integrated condenser-evaporator |
| $CSHP$ | chemisorption heat pump |
| $eq$ | equilibrium |
| $HX$ | heat exchanger |
| $i \rightarrow j$ | reaction from $i$ ammoniate to $j$ ammoniate |
| $liq$ | liquid ammonia in the condenser-evaporator |
| $salt$ | salt in the adsorber |
| $tot$ | total heat load |
| $vap$ | ammonia vapor |

## REFERENCES

Blackman, Corey, et al. 2019. "Study of optimal sizing for residential sorption heat pump system." Applied Thermal Engineering 150: 421-432.

Neveu, P. and J. Castaing, 1993. "Solid-gas chemical heat pumps: field of application and performance of the internal heat of reaction recovery process." Heat Recovery Systems & Chp.13(3): p. 233-251.

Tykodi, R., 1979. "Thermodynamics of Steady States: "Resistance Change" Transitions in Steady-state Systems." Bulletin of the Chemical Society of Japan 52(2): p. 564-570.

Li, T. X., R. Z. Wang, and H. Li, 2014. "Progress in the development of solid–gas sorption refrigeration thermodynamic cycle driven by low-grade thermal energy." Progress in Energy and Combustion Science 40: 1-58.

IECC, US Department of Energy, "Residential Prototype Building Models" [Internet], Available from: https://www.energycodes.gov/development/residential/iecc_models, accessed 7/24/2020

Energy Information Agency (EIA), "2015 residential energy consumption survey" [Internet], https://www.eia.gov/todayinenergy/detail.php?id=30672, accessed 7/24/2020

US Department of Energy, "Energy Data Facts" [Internet], https://rpsc.energy.gov/energy-data-facts, accessed 7/24/20